

## Thermoelastic properties of MgSiO<sub>3</sub> perovskite using the Debye approach

ORSON L. ANDERSON

Center for Physics and Chemistry of Planets, Institute of Geophysics and Planetary Physics, Department of Earth and Space Sciences, University of California at Los Angeles, Los Angeles, California 90095-1567, U.S.A.

### ABSTRACT

MgSiO<sub>3</sub> perovskite is shown to be a Debye-like mineral by the determination of specific heat,  $C_v$ , entropy,  $S$ , and thermal pressure,  $\Delta P_{Tn}$ , using the Debye theory up to 1800 K. Sound velocities and bulk moduli at ambient conditions published by Yeganeh-Haeri were used to find the ambient acoustic Debye temperature,  $\Theta_D^{ac}$ . The variation of  $\Theta_D^{ac}$  with  $T$  was assumed to be a curve parallel to the  $\Theta_D^{ac}$  vs.  $T$  curves previously found for Al<sub>2</sub>O<sub>3</sub>, MgO, and MgSiO<sub>3</sub>, enabling  $\Theta_D^{ac}(T)$  to be given up to 1800 K. To determine  $C_p$ , the thermal expansivity,  $\alpha$ , and the isothermal bulk modulus,  $K_T$ , are needed. After considering several sets of  $\alpha(T)$ , the  $\alpha(T)$  data of Funamori and his colleagues were chosen. Using the ambient  $K_T$  and the values of  $(\partial K_T/\partial T)_p$  vs.  $T$  reported by Jackson and Rigden,  $K_T(T)$  up to 1800 K was found. Then  $C_p(T)$  up to 1800 K was found assuming quasiharmonicity in  $C_v$ . The data behind the  $C_p(T)$  calculation are also sufficient to find the Grüneisen parameter,  $\gamma(T)$ , and the Anderson-Grüneisen parameters,  $\delta_T$  and  $\delta_S$ , up to 1800 K. The value of  $q = (\partial \ln \gamma/\partial \ln V)_T$  was found, and with  $\gamma$  and  $\rho$ ,  $\Delta P_{Tn}$  vs.  $V$  and  $T$  was determined. The three sound velocities,  $v_s$ ,  $v_p$ , and  $v_b = \sqrt{K_S/\rho}$ , were then determined to 1800 K. From  $v_s$  and  $v_p$ , Poisson's ratio and the isotropic shear modulus,  $G$ , were found to 1800 K. MgSiO<sub>3</sub> perovskite is one of a small, select group of Debye-like minerals for which thermoelastic properties and the equation of state (EOS) are calculable from acoustic data.

### INTRODUCTORY REMARKS ON DEBYE THEORY

Thermoelastic properties for a Debye solid, such as  $C_p$  vs.  $T$ , at  $P = 0$  can be easily calculated from standard Debye tables. A Debye solid is a monatomic solid (typically a metal) in which thermoelastic properties are a function of only one characteristic frequency,  $\omega_D$ , which is equivalent to one characteristic temperature,  $\Theta_D$  (Debye 1912). The specific heat,  $C_v$ , of a Debye solid is defined as (Kittel 1971)

$$C_v = 3R\mathcal{D}\left(\frac{\Theta_D}{T}\right) \quad (1)$$

where  $\Theta_D$  is the Debye temperature;  $R$  is the gas constant; and  $\mathcal{D}(\Theta_D/T)$  is the Debye function for specific heat found from tables. Most solids of interest to geoscience are not monatomic. Debye theory may be applied usefully to certain polyatomic minerals, provided the vibrational phonon density of states is well approximated by a Debye frequency spectrum (Kittel 1971),

$$\begin{aligned} g(\omega) &= a\omega^2 & \omega \leq \omega_D \\ &= 0 & \omega > \omega_D \end{aligned} \quad (2)$$

where  $\omega_D$  corresponds to  $\Theta_D$ .

Equation 2 does not work as a substitute for the phonon density of states if the solid has a wide band gap, as found in NaI,  $\alpha$ -quartz, or calcite. Polyatomic solids in which Equation 2 is a useful substitute for the phonon density

of states are called Debye-like solids; these include NaCl, MgO, Al<sub>2</sub>O<sub>3</sub>, and, as we shall see, MgSiO<sub>3</sub> perovskite. Minerals are rarely Debye-like solids because their thermoelastic properties are not usually a function of a single characteristic temperature. Note that there is no consideration of optic modes in a Debye-like solid.

The pertinent parameters are  $v_s$  and  $v_p$ , the shear and longitudinal sound velocities, and the maximum phonon frequency,  $\omega_D$  (or temperature,  $\Theta_D$ ). The value of  $\Theta_D$  is found from the sound velocities as given by the relation between  $\Theta_D$  and the mean sound velocity,  $v_m$  (Poirier 1991)

$$\Theta_D = 251.2 \left(\frac{\rho}{\mu}\right)^{1/3} v_m \quad (3)$$

where  $\mu = M/p$  is the mean atomic mass;  $M$  is the molecular mass;  $p$  is the number of atoms in the vibrating cell ( $p = 2$  for NaCl or MgO); and  $\rho$  is the density.  $v_m$ , the mean sound velocity, is related to the measured sound velocities by

$$\frac{3}{v_m^3} = \frac{2}{v_s^3} + \frac{1}{v_p^3} \quad (4)$$

$v_m$  is only slightly larger than  $v_s$ , as seen when Equation 4 is written as

$$v_m = v_s \left\{ \frac{3}{2 + (v_s/v_p)^3} \right\}^{1/3} \quad (5)$$

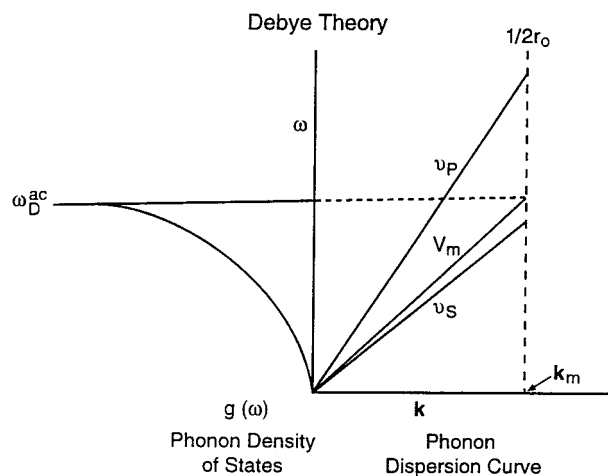


**FIGURE 1.** The phonon dispersion curve,  $\omega$  vs.  $\mathbf{k}$ , for a Debye solid that terminates at the maximum,  $1/2r_0$ . Under the assumptions of isotropy, there are two acoustic branches in a Debye solid, the upper one having a slope of  $v_p$  in kilometers per second and the lower one having a slope of  $v_s$  in kilometers per second. Debye theory requires an acoustic branch with the mean slope  $v_m$ , Equation 4. To the left are the phonon density of states,  $g(\omega)$ , vs.  $\omega$ , where the maximum frequency or Debye frequency,  $\omega_D^{\text{ac}}$ , is pinned to the maximum wave number,  $\mathbf{k}_m$ , at  $v_m$ .

(Anderson 1995). For typical ratios of ( $v_s/v_p$ ), say 0.6,  $v_m = 1.11 v_s$ . The acoustic frequencies are terminated at a wave number  $\mathbf{k}$  that is the reciprocal of the smallest interatomic spacing. In acoustic branches of the frequency dispersion curves, the slope of the  $\omega$ - $\mathbf{k}$  curve is the sound velocity.

These brief excerpts from Debye's theory emphasize that: (1) in this simple theory, there is no optic mode information; (2) the primary experimental information needed to apply the theory is the sound velocity (usually measured by an acoustic experiment); (3) the Debye theory applies to any temperature, provided the sound velocities and density are known at that temperature; and (4) the Debye temperature can be easily calculated from the acoustic sound velocities (Anderson 1963). For a Debye solid, the phonon-dispersion curve (a straight line), the frequency distribution (called the phonon density of states), and their relationship to each other are shown in Figure 1.

### DEBYE THEORY FOR POLYATOMIC SOLIDS

For polyatomic solids,  $p > 1$  and the original Debye assumptions are violated; hence the name Debye-like solids, when Equation 1 is empirically obeyed. NaCl is a good example of a Debye-like solid. The value of  $\Theta_D$  determined from acoustics is 316 K at low temperature, whereas the estimate of  $\Theta_D$  determined from calorimetric properties at high  $T$  is 321 K (Barron et al. 1980). The closeness in these values satisfies a requirement of Debye theory. The  $\omega$ - $\mathbf{k}$  dispersion curve calculated from lattice dynamics and the resulting  $f(\omega)$  curve for NaCl are plotted in Figure 2 (top), where the maximum lattice fre-

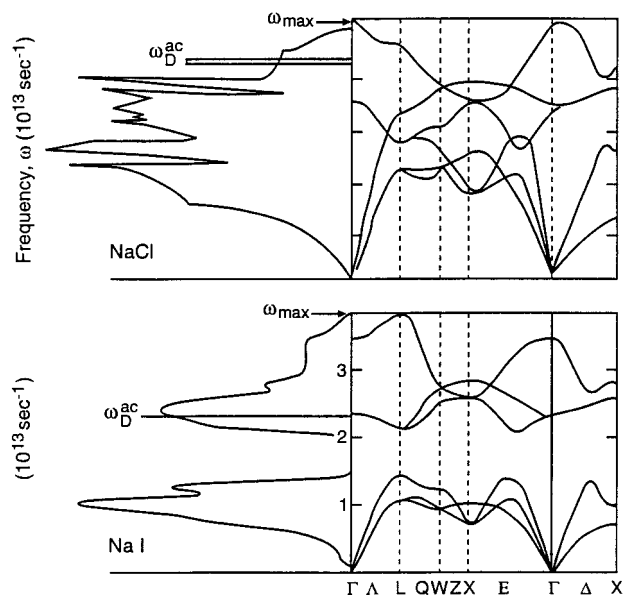


**FIGURE 2.** Three-dimensional phonon dispersion curves and the resulting density of states curves. (Top) NaCl showing the dispersion curves to the right and the phonon density of states to the left. The Debye frequency,  $\omega_D^{\text{ac}}$ , given by measured velocities of sound, is labeled as the line at the top. This shows that most values of  $\omega$  are less than  $\omega_D^{\text{ac}}$ ; hence NaCl is a Debye-like solid. (Bottom) NaI has a big band gap in  $\omega$  near the center of the spectrum. The line labeled  $\omega_D^{\text{ac}}$  is near the center of the density of states, and there are many modes whose frequency,  $\omega$ , is larger than  $\omega_D^{\text{ac}}$ . Hence NaI is not a Debye-like solid (modified from Birman 1984).

quency is  $\omega_{\text{max}}$ . Also shown is the position of  $\omega_D$  from acoustics, called  $\omega_D^{\text{ac}}$ , which is close to  $\omega_{\text{max}}$  for NaCl.

The Debye frequency spectrum,  $f(\omega)$ , is a parabola (Eq. 2) terminating at  $\omega_D^{\text{ac}}$  found from the experimentally determined  $v_m$  with an ordinate such that the area under the Debye curve is equal to the area under the actual phonon distribution curve,  $3pN$ . When the value of  $\omega_D^{\text{ac}}$  is close to that of the phonon dispersion determination of  $\omega_{\text{max}}$ , as shown in the top of Figure 2, the thermal properties calculated by Debye theory are close in value to corresponding measured values or to those calculated from the detailed phonon density of states.

NaI is an example of a solid that is not Debye-like. NaI has a wide band gap, and the frequency cutoff,  $\omega_{\text{max}}$ , is considerably larger than  $\omega_D^{\text{ac}}$  calculated from the acoustic properties, as shown in Figure 2 (bottom). The phonon density of states shows that almost half the modes have frequencies higher than  $\omega_D^{\text{ac}}$ . As a consequence, the specific heat curve,  $C_v$ , of NaI approaches the Dulong and Petit limit at much higher temperatures than predicted by the Debye theory.

Lattice dynamics deals with the vibrations of the whole lattice, three times Avogadro's number of vibrations. In this approach, the thermal energy is defined in a statistical sense (Born 1915, 1923; Barron 1955), and the thermoelastic properties are defined in terms of the lattice dynam-

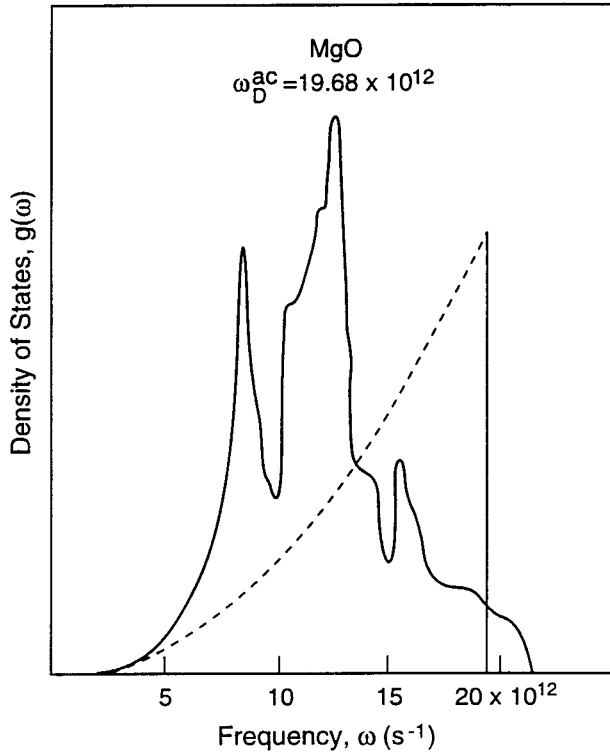


FIGURE 3. The Debye spectrum and the density of states for MgO. This solid is Debye-like because only a few frequencies are larger than  $\omega_D^{\text{ac}}$ , and the two spectra merge at low frequency. Density of states is from Sangster et al. (1970).

ical phonon density of states. A fairly good approximation to the phonon density of states can be represented by a histogram of cells using data constructed mainly from measured optic modes (Kieffer 1982, 1985). I call this the Kieffer method; it is really the crystallographic approach because it deals with the individual atoms in the crystallographic cell as the central basis for computing thermal energy of vibration. Each atom gives rise to three modes of vibration that are, in principle, identifiable by a spectroscopic measurement. In a few cases, the density of states can be effectively represented by a crude approximation, called the Debye spectrum, a quadratic curve with a sharp cutoff.

In contrast to the Kieffer method, the Debye theory assumes that all modes can be approximated by two different acoustic modes only, each having no dispersion, thus ignoring the optic modes. This assumption works for a few dense polyatomic solids in which almost all the optic modes have frequencies less than  $\omega_D^{\text{ac}}$ ; that is, if the optic modes are confined to the interior of the phonon density of states. For polyatomic solids in which many optic modal frequencies are large in comparison with  $\omega_D^{\text{ac}}$ , the Kieffer method is most useful.

In brief, a Debye-like solid is one in which the Debye spectrum maximum frequency,  $\omega_D^{\text{ac}}$ , as determined by the

TABLE 1. MgO: Comparison of  $C_V$  from Debye theory with  $C_V$  calculated by the measured  $C_p$

$T$ (K)	$\Theta_D^{\text{ac}}$ (K)	$\Theta_D^{\text{ac}}/T$	$C_V^{\dagger}$ Debye table [cal/ (mol·K)]	$C_V^{\ddagger}$ Debye [J/(mol·K)]	$C_V^{\S}$ from $C_p$ [J/(mol·K)]	$C_V^{\#}$ density of states [J/(mol·K)]
0	940					
400	937	2.343	4.397	36.820	42.274	41.590
500	928	1.856	5.045	42.247	42.234	44.491
600	920	1.533	5.311	44.474	45.880	46.023
700	911	1.301	5.480	45.889	46.466	47.030
800	902	1.128	5.594	46.844	46.990	47.675
900	894	0.993	5.673	47.506	47.350	48.118
1000	885	0.885	5.729	47.915	47.550	48.100
1100	875	0.796	5.772	48.334	47.750	48.682
1200	866	0.722	5.804	48.602	47.876	
1300	857	0.659	5.829	48.812	47.957	
1400	847	0.605	5.855	49.030	47.997	
1500	838	0.559	5.864	49.105	47.997	
1600	828	0.518	5.877	49.213	48.087	
1700	820	0.482	5.888	51.143	48.077	

\* $\Theta_D^{\text{ac}}$  from Table 30, Anderson and Isaak (1995).

$\dagger C_V$  (Debye table) from Table A-6.1, Anderson (1995): a monatomic solid ( $p = 1$ ).

$\ddagger C_V$  (Debye table) for a diatomic solid ( $p = 2$ ).

$\S C_V$  (from  $C_p$ ) from Table 15, Anderson and Isaak (1995).

$\# C_V$  (from phonon density of states) from Table 2, Chopelas (1990).

||Value of  $\Theta_D^{\text{ac}}$  reported by White and Anderson (1966), who also found  $\Theta_D^{\text{ac}} = 940$  K from lower temperature ( $T < 30$  K) thermal expansivity.

measured sound velocity, exceeds in value most of the optic frequencies in the phonon density of states.

### MgO: A DEBYE-LIKE SOLID

The case of MgO illustrates a Debye-like solid. Figure 3 shows the MgO phonon density of states (Sangster et al. 1970). On this plot is placed the Debye frequency,  $\omega_D^{\text{ac}}$ , determined by  $v_m$  ( $v_m$  having been determined by the isotropic averages of both  $v_p$  and  $v_s$ ). It is seen in Figure 3 that for the phonon density of states, the bulk of the optic modes is at frequencies between the high peak at  $13 \times 10^{12} \text{ s}^{-1}$  and  $\omega_D^{\text{ac}}$ , and only a small tail of frequencies exceeds  $\omega_D^{\text{ac}}$  ( $19.68 \times 10^{12} \text{ s}^{-1}$ ).

At absolute zero,  $\Theta_D^{\text{ac}}$  should be equal to the thermally determined Debye temperature,  $\Theta_D^{\text{th}}$ , at  $T = 0$  (Barron 1957). This is indeed the case for MgO. White and Anderson (1966) reported that at absolute zero,  $\Theta_D^{\text{ac}} = 940$  K, whereas  $\Theta_D^{\text{th}} = 946$  K. Also Barron (1957) showed that for a Debye solid  $\Theta_D^{\text{ac}}$  and  $\Theta_D^{\text{cal}}$  should be equal at high temperature. For MgO,  $\Theta_D^{\text{ac}}$  at 1200 K is 866 K, and Barron (1977) reported from his study of Debye-Waller factors that the calorimetric  $\Theta$  at infinite temperature ( $T > \Theta$ ) is near 810 K.

A crucial test for the existence of a Debye-like solid is to calculate  $C_V$  from the Debye theory, then compare it with  $C_V$  computed from the measured  $C_p$ , as done in Table 1 for MgO. Data on  $C_V$  from  $C_p$  from 400 to 1700 K in the table are taken from Table 15 in Anderson and Isaak (1995).  $C_V$  computed from the Debye theory, where the acoustic  $\Theta_D^{\text{ac}}$  descends slowly with  $T$ , is taken from Table 30 of Anderson and Isaak (1995). In this table we see that  $C_V$  from measured  $C_p$  differs from  $C_V$  calculated from

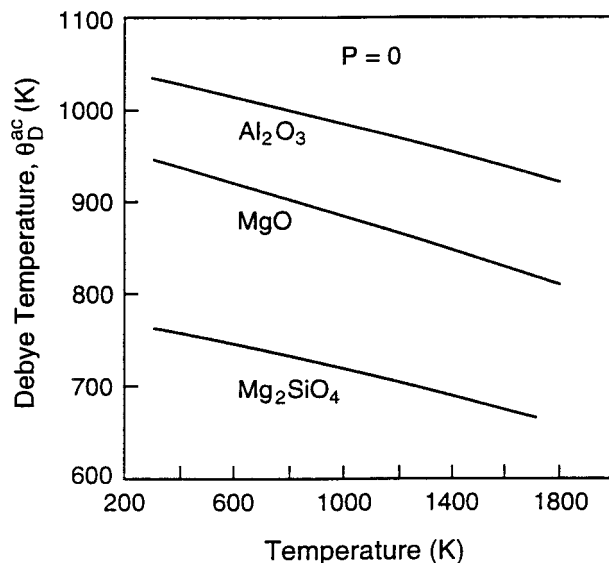


FIGURE 4. Debye temperature,  $\Theta_D^{\text{ac}}$ , vs.  $T$  for three oxide solids. These three plots show that  $\Theta_D^{\text{ac}}$  descends slowly with  $T$  and that the lines are parallel (data from Anderson and Isaak 1995).

acoustic velocities by less than about 2%, except for the end points.

Except for the end points, this error is within the experimental error of measured thermal expansivity, since

$$C_v = C_p - \alpha^2 K_T V T. \quad (6)$$

It is seen from Equation 6 that the conversion from  $C_p$  to  $C_v$  is sensitive to  $\alpha^2$ , so precise determination of  $\alpha$  is required to find the exact value of  $C_v$  from the measured  $C_p$ . Of all the variables measured in Equation 6,  $\alpha$  is often the least well known at high  $T$ . Excepting the values at 400 and 1700 K, the agreement is within about 2%. The disagreement at 400 K arises because the Debye theory is often weakest when  $T/\Theta < 0.4$ . This is where the Debye  $C_v$  curve is rising rapidly with  $T$ , and a small error in  $T/\Theta$  is greatly multiplied to make the uncertainty in  $C_v$  ( $T/\Theta$ ) large. The disagreement at 1700 K arises from the uncertainty in the measured  $\alpha$  at that  $T$ . The overall agreement between  $C_v$  (Debye) and  $C_v$  (from  $C_p$ ) is as good as can be found for most metals and is satisfactory proof that MgO is a Debye-like solid.

In the last column of Table 1 are listed the values of  $C_v$  calculated by Chopelas (1990) from the phonon density of states, as given by Sangster et al. (1970) and shown in Figure 3. The equation used to find  $C_v$  as a function of  $T$  using the phonon density of states,  $g(\omega)$ , is

$$C_v = 3pR \int_0^\infty \frac{e^x}{(e^x - 1)} x^2 g(\omega) d\omega \quad (7)$$

where  $x = (h\omega)/(kT)$ . The comparison between  $C_v$  as calculated by the Debye theory,  $C_v$  determined by the experimental data on  $C_p$ , and  $C_v$  from the density of states (Eq. 7), is shown in Table 1.

The main feature of the calculation of  $\Theta_D$  for MgO is

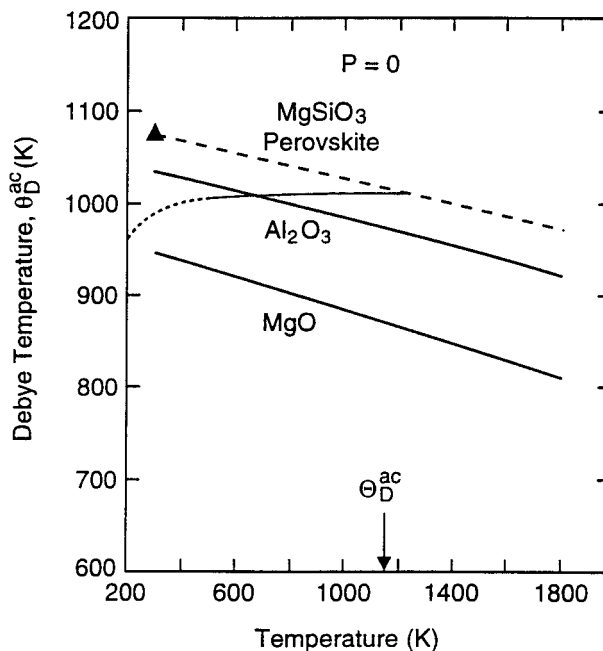


FIGURE 5. Debye temperature,  $\Theta_D^{\text{ac}}$ , vs.  $T$  for MgSiO<sub>3</sub> perovskite. The value,  $\Theta_D^{\text{ac}} = 1080$  K, is anchored at  $T = 300$  K by the acoustic experiments of Yeganeh-Haeri (1994). The  $\Theta_D^{\text{ac}}$  curve is made parallel to the Al<sub>2</sub>O<sub>3</sub> and MgO lines. The dotted line represents the calorimetric determination of  $\Theta$ ,  $\Theta_D^{\text{cal}}$ , by Akaogi and Ito (1993), and their extrapolation to high  $T$  is shown by the light solid line.

the steady decrease of  $\Theta_D^{\text{ac}}$  with temperature resulting from the temperature dependence of the sound velocities (plotted in Fig. 4). I depart from customary procedure in that the acoustic data here appropriate to every temperature are used to determine the value of  $\Theta_D^{\text{ac}}$  and in the calculation of  $C_v$  at that temperature. Also plotted in Figure 4 is  $\Theta_D^{\text{ac}}$  vs.  $T$  for two other solids: Al<sub>2</sub>O<sub>3</sub> and Mg<sub>2</sub>SiO<sub>4</sub>. Note that the slopes of  $\Theta_{\text{ac}}$  vs.  $T$  are similar for all three minerals.

The assumed variation of  $\Theta_D^{\text{ac}}$  with  $T$  for MgSiO<sub>3</sub> perovskite is shown in Figure 5, plotted as a dashed line. The slope of MgSiO<sub>3</sub> vs.  $T$  is made parallel to the measured slopes of Al<sub>2</sub>O<sub>3</sub> and MgO. The triangle plotted in Figure 5 is from the Brillouin measurements of Yeganeh-Haeri (1994), giving  $v_s$  and  $v_p$ , which anchor the low- $T$  end of  $\Theta_D^{\text{ac}}(T)$ . Using specific heat data, Akaogi and Ito (1993) estimate  $\Theta_D^{\text{cal}}$  and its variation with  $T$  from 100 to 400 K, as shown by the dotted line in Figure 5. The Akaogi and Ito estimated value for  $\Theta_D^{\text{cal}}$  at 1000 K is 1030 (20), agreeing well with the value for  $\Theta_D^{\text{ac}} = 1027$  K at 1000 K.

### MgSiO<sub>3</sub> PEROVSKITE: ANOTHER DEBYE-LIKE SOLID The phonon density of states of MgSiO<sub>3</sub> perovskite

The Debye theory customarily is assumed to apply to MgSiO<sub>3</sub> perovskite whenever the thermal energy factor,  $E_{\text{th}}$ , in the Mie-Grüneisen expression for thermal pressure

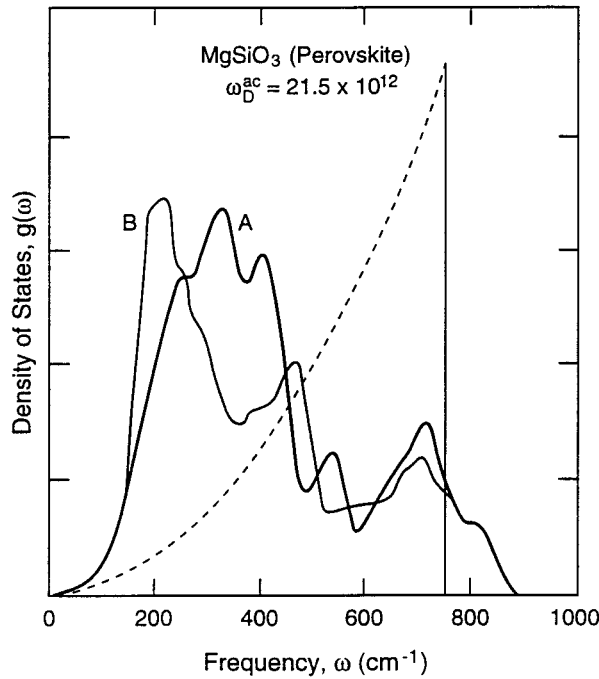


FIGURE 6. The phonon density of states for MgSiO<sub>3</sub> perovskite: (A) from Choudhury et al. (1988) and (B) from Winkler and Dove (1992). These are compared with the Debye spectrum, where  $\omega_D^{ac} = (\hbar/k)\Theta_D^{ac}$ . As in the case of MgO (Fig. 3), only a small portion of the spectrum has frequencies higher than  $\omega_D^{ac}$ , and the Debye spectrum and the density of states merge at low frequency. This is evidence that MgSiO<sub>3</sub> perovskite is a Debye-like solid.

is calculated by the Debye function for internal energy (as was done by Stixrude et al. 1992 and Jackson and Rigden 1996).

Liebermann (1982) calculated successfully the bulk sound velocity,  $v_b$ , of MgSiO<sub>3</sub> perovskite by the formula,  $v_b \mu^{1/2} = \text{constant}$ , which was derived by Shankland (1972) from Debye theory. The idea that MgSiO<sub>3</sub> perovskite may be a Debye-like solid is certainly not new (Anderson 1995), but it has not yet been proved.

Thus I examine evidence that MgSiO<sub>3</sub> perovskite is a Debye-like solid. The phonon density of states for MgSiO<sub>3</sub> perovskite according to two sets of calculations (Choudhury et al. 1988; Winkler and Dove 1992) is shown in Figure 6. These phonon densities of states are different. The difference does not significantly affect the Debye approximation to the phonon density of states, but it does affect the calculation of moments of the spectrum, so the moment method used to find  $\Theta_D$  (Anderson 1995) is not to be used for MgSiO<sub>3</sub> perovskite.

The density of states of MgSiO<sub>3</sub> perovskite is similar to that of MgO in two important features. First, the frequencies of the phonon density of states of MgSiO<sub>3</sub> perovskite are, for the most part, less than  $\omega_D^{ac}$ , with only a small tail of the spectrum lying beyond the acoustic  $\omega_D^{ac}$ . Second, at low frequencies, the quadratic frequency de-

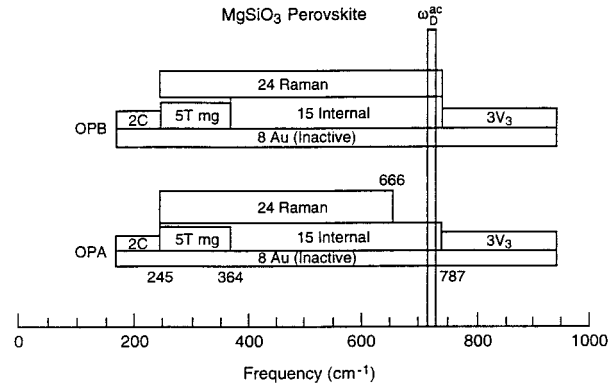


FIGURE 7. The phonon density of states for MgSiO<sub>3</sub> perovskite constructed from optic modes (the Kieffer approach) by Lu et al. (1994). Note again that the majority of the modes have frequencies less than  $\omega_D^{ac}$ .

pendence of the Debye spectrum merges into the solid's phonon density of states. Note that MgSiO<sub>3</sub> perovskite satisfies the quadratic fit at low  $\omega$  about as well as does MgO. Therefore we can expect the properties of MgO arising from Debye theory to be a guide for the corresponding properties of MgSiO<sub>3</sub> perovskite.

Figure 7 shows the density of states model of MgSiO<sub>3</sub> perovskite given by Lu et al. (1994). This is a Kieffer-style density of states constructed from data on measured optic modes. This plot shows the position of  $\omega_D^{ac}$  as determined by the velocity measurements of Yeganeh-Haeri (1994), which is 720 cm<sup>-1</sup>. This plot shows that the preponderance of optic modes lies near the mid-region of the spectrum and that few have frequencies larger than  $\omega_D^{ac}$ . This is further evidence that MgSiO<sub>3</sub> perovskite is likely to be a Debye-like solid. The results of  $C_V(T)$  found by using the  $\Theta_D^{ac}(T)$  curve are shown in columns 3 and 4 of Table 2.

From this table it is seen that the Debye values of  $C_V$  for MgSiO<sub>3</sub> perovskite at 300 and 1000 K are 70.66 J/(mol·K) and 118.48 J/(mol·K). The values (in the same units) at the same temperatures reported by Winkler and Dove (1992) are 85.29 and 119.97. They used Equation 7 with their phonon density of states, shown in Figure 6. This further indicates that the Debye model is fairly good for the quasiharmonic calculation of  $C_V$ , provided one focuses on temperatures above 400 K. Data on  $C_V$  of MgSiO<sub>3</sub> perovskite are sparse in the literature, because  $C_p$  apparently has not been measured above 300 K (Akaogi and Ito 1993).

#### Calculation of $C_p(T)$ emphasizing the importance of $\alpha(T)$

Experimental data on  $C_p(T)$  of MgSiO<sub>3</sub> perovskite over a limited range of  $T$  have been presented by Akaogi and Ito (1993). Comparison of  $C_p$  with the Debye model calculations, which give  $C_v$ , requires evaluation of the  $\alpha^2 K_T VT$  correction term in Equation 6. Calculations of  $C_p$  from  $C_v$  are presented in Table 3. Note that at high  $T$ ,  $C_p$  from this report is substantially lower than that reported

**TABLE 2.** MgSiO<sub>3</sub> perovskite:  $C_V$  and  $C_p$ 

$T$ (K)	$\Theta_D^c$ (K)	$C_V^*$ Debye [cal/ (mol·K)]	$C_V^\dagger$ Debye [J/ (mol·K)]	$C_p^\ddagger$ This Report [J/(mol·K)]	$C_p^\S$ Saxena [J/ (mol·K)]	$C_p^\#$ Chop- elas (J/mol·K)	$C_p^\parallel$ Lu et al. (J/ mol·K)
300	1076	3.376	70.66	78.6**	80.3	82.7	74.9
400	1069	4.273	89.59	90.6	90.5	98.1	92.1
500	1062	4.805	100.22	101.7	107.7	107.2	103.4
600	1055	5.079	106.74	108.9	114.3	113.0	111.1
700	1048	5.339	111.20	114.1	119.5	116.9	116.9
800	1041	5.482	114.46	118.0	124.0	119.8	121.5
900	1034	5.581	116.83	120.8	127.9	122.1	125.5
1000	1027	5.653	118.48	122.9	131.4	123.9	129.1
1100	1020	5.708	119.57	124.6	134.5		132.6
1200	1013	5.749	120.33	126.1	137.3		136
1300	1006	5.781	120.94	127.5	139.9		139.4
1400	999	5.888	121.54	128.7	142.3		142.9
1500	992	5.828	122.08	129.5	144.5		146.4
1600	985	5.845	122.44	130.4	146.6		150.1
1700	978	5.859	122.57	131.5	148.5		153.8
1800	971	5.871	122.93	132.4	150.4		157.7

Note: Funamori et al. (1996) values of  $\alpha$  and  $V$  used for correction from  $C_V$  to  $C_p$ . Comparison of calculated  $C_p$  with other authors. For value of  $C_p - C_V = \alpha^2 K_T V T$ , see Table 4.

\* $C_V$  (Debye)  $p = 1$  from the standard Debye table.

† $C_V$  (Debye)  $p = 5$ : conversion from  $C_V$  (Debye)  $p = 1$  to the case of MgSiO<sub>3</sub> perovskite.

‡ $C_p$  (Debye)  $p = 5$  obtained by using  $C_p - C_V$  corrections listed in Table 3.

§ $C_p$ : as determined by Saxena et al. (1993) using  $\alpha$  and  $V$  from Knittle et al. (1986).

# $C_p$ : as determined by Chopelas et al. (1994) using a Kieffer-like density of states.

|| $C_p$ : as determined by Lu et al. (1994) using a Kieffer-like density of states and  $\alpha$  from Mao et al. (1991).

\*\* $C_p$  (experiment) at 300 K = 80.6 J/(mol·K) (Akaogi and Ito 1993).

by Saxena et al. (1993) and by Lu et al. (1994). The difference comes from different values of  $\alpha$  used in the correction term, which is sensitive to  $\alpha^2$ . This difference justifies a discussion on the appropriate values of  $\alpha$  that should be used for MgSiO<sub>3</sub> perovskite at high  $T$ .

At the time the Saxena et al. (1993) book and the Lu et al. (1994) paper were written, the values of  $\alpha$  for (Mg,Fe)SiO<sub>3</sub> perovskite from Knittle et al. (1986) and Mao et al. (1991) were virtually unchallenged, and so they were used by these authors.

But shortly after the publication of these two reports, many experimental papers on  $\alpha$  of MgSiO<sub>3</sub> perovskite were published (Wang et al. 1994; Utsumi et al. 1995; Funamori et al. 1996). Masuda and Anderson (1995), using the Utsumi et al. (1995) experimental data to evaluate parameters of the Suzuki equation, found  $\alpha(T)$ . Jackson and Rigden (1996) reported a  $PVT$  study of the combined data of Ross and Hazen (1989), Wang et al. (1994), Utsumi et al. (1995), and Funamori et al. (1996), and they recommended values of  $\alpha$  for  $\alpha(T)$ . Chopelas (1996) and Gillet et al. (1996a) found  $\alpha(T)$  from their spectroscopic measurements. Anderson et al. (1996) used the Funamori et al. (1996) data on  $V(T)$  for MgSiO<sub>3</sub> to find  $\alpha(T)$  for MgSiO<sub>3</sub>; the data are listed in Table 3, column 5. All the results for  $\alpha(T)$  published by the authors listed in this paragraph essentially agree with one another, and all are substantially lower than the data presented earlier by Knittle et al. (1986) and Mao et al. (1991). These com-

**TABLE 3.** Details of calculation of  $C_p - C_V$  correction

$T$ (K)	Funamori* $\alpha \times 10^5$ (K <sup>-1</sup> )	Knittle† $\alpha \times 10^5$ (K <sup>-1</sup> )	$K_T^\ddagger$ (GPa)	Funamori§ $V$ (cm <sup>3</sup> /mol)	Knittle# $V$ (cm <sup>3</sup> /mol)	This report $C_p - C_V$ (J/mol·K)	For Knittle $C_p - C_V$ (J/mol·K)
500	2.18	3.39	257.9	24.56	24.6	1.5	3.7
600	2.45	3.67	255.4	24.58	24.7	2.3	5.1
700	2.58	3.88	252.8	24.68	24.8	2.9	6.6
800	2.63	4.06	250.2	24.78	24.9	3.4	8.1
900	2.68	4.22	247.6	24.82	25.0	4.0	9.8
1000	2.70	4.36	244.9	24.88	25.1	4.4	11.6
1100	2.74	4.50	242.2	24.94	25.2	5.0	13.4
1200	2.83	4.63	239.5	25.04	25.4	5.8	15.4
1300	2.90	4.76	236.8	25.14	25.5	6.5	18.2
1400	2.91	4.88	234.0	25.21	25.6	7.1	19.6
1500	2.93	5.00	231.0	25.28	25.7	7.5	21.9
1600	2.94	5.12	228.5	25.36	25.9	7.9	24.4
1700	2.95	5.24	225.7	25.41	26.0	8.9	26.8
1800	3.00	5.36	223.0	25.49	26.1	9.4	29.6

Note:  $C_p - C_V$  correction =  $\alpha^2 K_T V T$ .

\* $\alpha$  from Anderson et al. (1996) using Funamori et al. (1996) data.

† $\alpha$  from Saxena et al. (1993) using Knittle et al. (1986) basic data on  $\alpha$ .

‡ $K_T$  at 300 K from Jackson and Rigden (1996) derived from  $K_S$  at 300 K measured by Yeganeh-Haeri (1994). Dependence on  $T$  given by  $(\partial K_T / \partial T)_p$  presented by Jackson and Rigden (1996).

§ $V$  from Utsumi et al. (1995) and Funamori et al. (1996).

# $\Delta V$  from Saxena et al. (1993) using Knittle et al. (1986) basic data on  $\alpha$  and  $V$ .

parisons of  $\alpha(T)$  are illustrated in Figure 8. The value used here (see Table 3),  $\alpha = 2.58 \times 10^{-5}$  at 800 K, compares well with the Gillet et al. (1996a) value,  $\alpha = 2.5 \times 10^{-5}$  at 800 K.

The evaluation of the correction term,  $C_p - C_V = \alpha^2 K_T V T$ , is shown in Table 3, in which the values of  $\alpha$ ,  $K_T$ , and  $V$  are given in detail. It is seen from Table 3 that the correction term when using the Knittle et al. (1986)  $\alpha$  data is three times larger at 1600 K than the correction term when using the Funamori et al. (1996)  $\alpha$  data.

The value of  $K_T$  used in computing the correction term here (column 2, Fig. 3) is found by integrating  $(\partial K_T / \partial T)_p$  vs.  $T$  as presented by Jackson and Rigden (1996). This is discussed in detail later.

The value of  $C_V$  from the Debye model is shown in column 4 of Table 2; it has reached the Dulong and Petit limit at 1800 K. Because the  $C_p - C_V$  correction is known for the respective  $\alpha$  data, one can check on whether the various  $C_p$  calculations use an underlying quasi-harmonic  $C_V$ . They all do. Gillet et al. (1996a) investigated the possible presence of anharmonicity by finding the effect of temperature on the Raman spectrum of MgSiO<sub>3</sub> perovskite up to 300 K and concluded that there was no evidence of intrinsic anharmonicity strong enough to affect the equation of state, even at very high temperatures (see also Gillet 1996). I conclude, therefore, that anharmonicity need not be considered in the expression for the high-temperature  $C_V$ , and that MgSiO<sub>3</sub> perovskite is indeed quasi-harmonic. Calcite, on the other hand, is a solid for which an anharmonicity component is required in the  $C_V$  analysis (Gillet et al. 1996b). The various  $C_V$  models discussed here appear to be similar, but the  $C_p - C_V$  correction varies depending on the choice of  $K_T(T)$  and  $\alpha(T)$ .

In spite of the fact that the  $C_p - C_v$  correction obscures the value of  $C_v$  for the last three columns in Table 2, the Debye model appears to perform as well as the other models arising from the density of states, which use varieties of the Kieffer spectrum.

### Calculation of entropy

Navrotsky (1989) used the simplest approximation for the MgSiO<sub>3</sub> perovskite density of states, a simple, one-continuum model, a rectangular box, between 225 and 900 cm<sup>-1</sup>, and she found that this model led to  $S = 180.9$  J/(mol·K) at 1000 K. Gillet et al. (1993) replaced Navrotsky's one-continuum model with a two-cell continuum, and from this calculated  $S$  and  $C_p$  for MgSiO<sub>3</sub> perovskite between 225 and 900 cm<sup>-1</sup> (a Kieffer approach) and found 235–247 J/mol for the entropy at 1100 K. I calculated 193 J/mol at 1100 K by the Debye method (see Table 4). The Gillet et al. (1993) value of  $C_p$  was 135–136.7 J/(mol·K) at 1100 K; this should be compared with 124.6 J/(mol·K) at 1100 K shown in Table 2. Akaogi and Ito (1993) reported that by using their experimental determinations of  $C_p$ , the entropy of MgSiO<sub>3</sub> perovskite is found to be 57.2 J/mol and 185.5 J/mol at 298 and 1000 K, respectively.

I found  $S(300)$  from  $\int_0^{300} (C_p/T) dT$  for the range of  $T$  below 300 K using the  $C_p$  data of Akaogi and Ito (1993) measured between 140 and 295 K. By using a short extrapolation near absolute zero, it was found that  $S(300) = 57.4 \pm 4$  J/mol for MgSiO<sub>3</sub> perovskite, close to the Akaogi and Ito (1993) result mentioned above. Thus in my calculation

$$S(T) = \int_0^T \frac{C_p}{T} dT = 57.4 + \int_{300}^T \frac{C_p}{T} dT \text{ J/mol.} \quad (8)$$

The values of  $S(T)$  so calculated are shown in Table 4 under the column heading  $S^{**}(\text{Debye})$  and in its note ( $p = 5$ ). The values of  $S(T)$  reported here also agree well with the reports of Chopelas et al. (1994) and Lu et al. (1994), in that the Debye values are between the other two values, which were based on Kieffer-type models. Thus there is reasonable agreement between the  $S(T)$  from experiment and the  $S(T)$  calculated from  $C_p$  (in turn calculated from the Debye  $C_v$ ). Differences in entropy have as an underlying cause the difference in thermal expansivity used in the calculation of the  $C_p - C_v$  correction, as well as different approximations for the density of states.

### CONTROVERSIES OVER $\alpha(T)$ AND $(\partial K_T/\partial T)_p$

#### The low sets of $\alpha(T)$ vs. the high sets of $\alpha(T)$

The value of  $\alpha(T)$  chosen from the set of  $\alpha(T)$  values available for MgSiO<sub>3</sub> perovskite has a strong effect on the values of entropy and specific heat, as shown above. The choice of  $\alpha(T)$  has a strong effect on the predicted density distribution of perovskite at lower mantle conditions as well (Jackson 1983; Stixrude et al. 1992).

In the upper set of values of  $\alpha(T)$  found in Figure 8

**TABLE 4.** Comparison of entropy at ambient pressure calculated from the Debye model and calculations from Kieffer-like density of states for MgSiO<sub>3</sub> perovskite with vibrational modes

$T$ (K)	$\Theta_D/T$	$S^*$ Debye (J/mol)	$S^\dagger$ Lu et al.	$S^\ddagger$ Chopelas et al.
150	7.233	18.3		16.6
200	5.415	30.8		30.0
250	4.320	44.1		44.2
300	3.587	57.4	51.4	58.2
400	2.673	80.9	74.9	84.3
500	2.124	102.5	96.1	107.2
600	1.758	121.7	115.0	127.3
700	1.497	138.9	131.7	145.0
800	1.301	154.4	146.7	160.9
900	1.149	168.5	160.3	175.1
1000	1.027	181.3	172.5	188.1
1100	0.927	193.1	183.8	
1200	0.844	204.0	194.2	
1300	0.774	214.1	203.8	
1400	0.714	223.6	212.7	
1500	0.661	232.5	221.1	
1600	0.616	240.9	228.4	
1700	0.575	248.9	236.3	
1800	0.539	256.4	243.3	

Note: Same as bottom of Table 3,  $S(\text{Debye}) p = 1$ .  $S(\text{Debye}) p = 1$  from the standard Debye table.

\* $S(\text{Debye}) p = 5$  conversion of  $S(\text{Debye}) p = 1$  to the case of Mg<sub>2</sub>SiO<sub>4</sub> perovskite.

† $S$  Lu et al. (1994) a Kieffer-like density of states model.

‡ $S$  Chopelas et al. (1994) a Kieffer-like density of states model.

are those found by Knittle et al. (1986) for Fe-rich MgSiO<sub>3</sub> perovskite, as reported by Saxena et al. (1993) in a table labeled "MgSiO<sub>3</sub> perovskite," and those found by Mao et al. (1991) for an Fe-rich MgSiO<sub>3</sub> perovskite, as graphed by Chopelas (1996). In the lower sets of  $\alpha(T)$  in Figure 8, the data are all for pure MgSiO<sub>3</sub> perovskite (with no Fe). On this basis, one should choose  $\alpha(T)$  measured on a non Fe-bearing MgSiO<sub>3</sub> perovskite to calculate  $C_p$  and entropy for a non Fe-bearing MgSiO<sub>3</sub>.

I note, however, the importance of the magnitude of  $\alpha(T)$  in determining the composition of the lower mantle. Both Jackson (1983) and Jeanloz and Knittle (1989) emphasized that a large value of  $\bar{\alpha}$  between 300 and 1700 K leads to a chondritic-like lower mantle, hence not a pyrolytic mantle composition. Zhao and Anderson (1994) showed that the  $\alpha$  values reported by Mao et al. (1991), in contrast to the  $\alpha$  data of Wang et al. (1994), lead to "drastic differences in the fraction of silicate perovskite in a two phase-mixture lower mantle."

#### The high value or the low value of $|(\partial K_T/\partial T)_p|$ for silicate perovskite?

The experimental values of  $(\partial K_T/\partial T)_p$  vs.  $T$  are needed to find extrapolated values of the bulk modulus in this paper, in particular, column 4 of Table 3. This brings us squarely against the controversy about this parameter: Authors measuring this parameter are grouped just as in Figure 8. Those whose data on  $\alpha(T)$  are in the upper set of Figure 8 also report a large value of  $|(\partial K_T/\partial T)_p|$ , where-

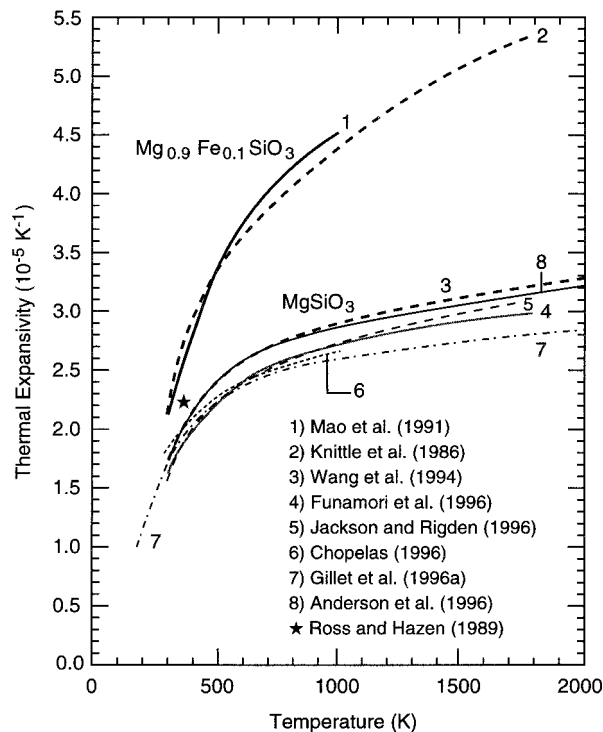


**FIGURE 8.** Thermal expansion,  $\alpha$ , curves from experiments or the analysis of experiments. Note that the curves are sorted into two groups. The upper group of two curves shows a high value of  $\alpha$  at high  $T$ . The lower group of six curves shows a much lower value of  $\alpha$  at high  $T$ . The lower group represents the most current work. The lower group of  $\alpha(T)$  curves results in  $\text{MgSiO}_3$  having a larger density at lower mantle conditions than the lower mantle itself and thus favors a pyrolytic composition for the lower mantle. The upper group of  $\alpha(T)$  curves yields a density at lower mantle conditions that, with little adjustment, matches the lower mantle density.

as those authors whose data occupy the lower sets have values about half as large (see Table 5).

The calculation of the  $C_p - C_v$  correction and entropy requires an accurate value of  $K_T$  at high temperature, and to find  $K_T$  requires an accurate value of  $(\partial K_T/\partial T)_p$  because measurements of  $K_s$  or  $K_T$  do not exist at high  $T$ . For  $\text{MgSiO}_3$  perovskite, the values of  $(\partial K_T/\partial T)_v$  are reported between  $-0.020$  and  $-0.028$  GPa/K, with the exception of the Stixrude et al. (1992) value,  $-0.060$  GPa/K, on the basis of the Mao et al. (1991) data. I believe the value of  $|(\partial K_T/\partial T)_p|$  reported by Stixrude et al. (1992) is much too high. If the Stixrude et al. value of  $(\partial K_T/\partial T)_p = -0.06$  GPa/K is used,  $K_T(T)$  of perovskite descends very rapidly with  $T$ , and, at temperatures corresponding to deep within the lower mantle,  $K_T(T)$  of  $\text{MgSiO}_3$  perovskite might approach  $K_T(T)$  of  $\text{MgO}$  (see Fig. 9 of Anderson et al. 1996).

Even when neglecting the Stixrude et al. value, there is still a difference between values of  $(\partial K_T/\partial T)_p$  listed in Table 5. I believe this is due to the fact that below the Debye temperature, the value of  $|(\partial K_T/\partial T)_p|$  decreases

**TABLE 5.** High-temperature derivatives of the isothermal bulk modulus,  $K_T$

Experimental reports	$(\partial K_T/\partial T)_p$ GPA $\text{K}^{-1}$
<b>MgO</b>	
Anderson et al. (1992)	-0.031
<b><math>\text{Al}_2\text{O}_3</math></b>	
Anderson et al. (1992)	-0.030
<b><math>\text{Mg}_2\text{SiO}_4</math></b>	
Anderson et al. (1992)	-0.023
<b>Olivine</b>	
Anderons et al. (1992)	-0.022
<b><math>\text{MgSiO}_3</math> Perovskite</b>	
Wang et al. (1994)	-0.023
Anderson and Masuda (1994)	-0.026
Utsumi et al. (1995)	-0.030
Funamori et al. (1996)	-0.028
Jackson and Rigden (1996) $T \approx 300$ K	-0.021
Jackson and Rigden (1996) $T > \theta$	-0.028
Stixrude et al. (1992)	-0.060
Mao et al. (1991)	-0.063

steadily with decreasing  $T$  and eventually approaches zero at  $T = 0$ , similar to the behavior of  $C_p$  at  $T$  close to zero. I have used the graph showing  $(\partial K_T/\partial T)_p$  over a wide temperature range presented by Jackson and Rigden (1996) as the basis for Figure 9, which is adapted from their Figure 6, to emphasize this point.

Authors whose data on  $\alpha$  emphasize the lower temperatures report a lower value of  $|(\partial K_T/\partial T)_p|$  than do the authors whose data emphasize the upper temperatures. I used the curves of  $(\partial K_T/\partial T)_p$  and  $(\partial K_s/\partial T)_p$  in Figure 9 to find by integration  $K_T(T)$  and  $K_s(T)$  from Yeganeh-Haeri's (1994) values of  $K_s$  and  $K_T$  at 300 K. The values so determined are listed in Tables 3 and 6.

#### ADDITIONAL THERMOELASTIC PROPERTIES OF $\text{MgSiO}_3$ PEROVSKITE

With the tabled values of  $K_T$ ,  $K_s$ , as well as  $\alpha$  available as a function of  $T$ , there are sufficient data for the determination of the Anderson-Grüneisen parameters,

$$\delta_T = -\left(\frac{1}{\alpha K_T}\right)\left(\frac{\partial K_T}{\partial T}\right)_p \quad (9)$$

and

$$\delta_s = -\left(\frac{1}{\alpha K_s}\right)\left(\frac{\partial K_s}{\partial T}\right)_p \quad (10)$$

The values of these parameters are listed in Table 6, columns 3 and 4.  $K'_0(T)$  can be evaluated at 100 K intervals with the help of the value of  $(\partial^2 K_T/\partial T^2)_p$ , found by Jackson and Rigden (1996),  $1.4 \times 10^{-4} \text{ K}^{-1}$ . Thus

$$K'_0(T) = K'_0(300) + 1.4 \times 10^{-4}(T - 300). \quad (11)$$

Values of  $T$  are listed in column 5, Table 6. The Grüneisen ratio,  $\gamma = \alpha K_T V / C_v$ , is next evaluated and listed in column 6 of Table 6.



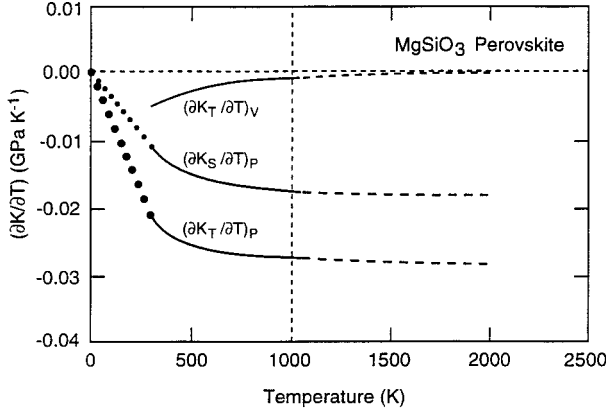


**FIGURE 9.** Values of the temperature derivatives of the bulk modulus vs.  $T$  for MgSiO<sub>3</sub> (modified from Fig. 6 of Jackson and Rigden 1996). Solid lines represent the range of available PVT data. Dashed lines represent extrapolations. Dotted lines represent the author's interpolation to absolute zero. It is to be noted that there is considerable variation in  $(\partial K_S/\partial T)_P$  and  $(\partial K_T/\partial T)_P$  between 300 K and about 800 K. It is also to be noted that  $(\partial K_T/\partial T)_V$  approaches zero just beyond  $\Theta$ .

The value of  $q = (\partial \ln \gamma / \partial \ln V)$  can be evaluated from the equation (Anderson 1995).

$$q = \delta_T - K' + 1 \left( \frac{\partial \ln C_V}{\partial \ln V} \right)_T \quad (12)$$

At  $T > \Theta$ , the  $(\partial \ln C_V / \partial \ln V)$  term vanishes, so that for  $T \approx \Theta$ , Table 6 shows that  $\delta_T$  is close to  $K'_0$ , and thus  $q$  is very close to unity.

The value of  $v_s$  is determined from  $\Theta_B^{ac}$  by means of Equations 3 and 4 and  $v_b$  from  $K_S$  and  $\rho$ , where  $K_S$  comes primarily from the Jackson and Rigden (1996) determination of  $(\partial K_S/\partial T)_P$ , and  $\rho$  comes from the Funamori et al. (1996) data on  $V(T)$ . Through  $v_b$  and  $v_s$ ,  $v_p$  is determined by  $v_p^2 = K/\rho + 4/3 v_s^2$ . The variation of Poisson's ratio with  $T$  is calculated from  $v_s$  and  $K/\rho$ . It is seen from Table 7 that  $\sigma$  varies between 0.224 and 0.238 from 300 to 1800 K, similar to the variation of  $\sigma$  in Al<sub>2</sub>O<sub>3</sub> (Anderson and Isaak 1995). The value of the isotropic shear modulus, determined from  $G = \rho v_s^2$ , is listed in Table 7.

#### THERMAL PRESSURE IN THE EQUATION OF STATE

In PVT calculations where a thermal equation of state is used, the contribution to temperature effects comes from the thermal pressure,  $\Delta P_{Th}$ . At high  $T$  in the quasi-harmonic approximation,  $P_{Th}$  is proportional to  $T$ , and the proportionality parameter is  $\alpha K_T$  (Anderson 1995).

The equation to obtain the thermal pressure using  $\alpha K_T$  (Anderson and Zou 1989), where  $P_{Th}$  is a function of  $V$  and  $T$ , is

$$\Delta P_{Th} = \alpha K_T (T - T_0) - (\partial K_T / \partial V)_V \ln \frac{V}{V_0} \quad (13)$$

Jackson and Rigden (1996) correctly pointed out that to obtain  $\Delta P_{Th}$  in  $P$ - $T$  space, Equation 13 is not rigorously

**TABLE 6.** Dimensionless thermoelastic parameters and thermal pressure parameters for MgSiO<sub>3</sub> perovskite, arising from the Debye model

$T$ (K)	$K_S^*$ Adia- batic bulk mod. (GPa)	$\delta_T \dagger$	$\delta_S \ddagger$	$K'_0 \S$	$\gamma \#$	$q^\ddagger$	$\alpha K_T \parallel$ (MPa)	$\Delta P_{Th}^{**}$ Thermal pressure (GPa)
300	264.0			4.00	1.52		4.38	0
400	262.8	4.98	4.14	4.014	1.41	(1.39)	5.13	0.47
500	262.0	4.87	3.94	4.028	1.37	(1.34)	5.62	1.015
600	260.7	4.78	3.92	4.042	1.39	(1.34)	6.03	1.597
700	259.2	4.65	3.84	4.056	1.38	(1.29)	6.24	2.210
800	258.0	4.40	3.81	4.076	1.40	(1.12)	6.46	2.846
900	256.9	4.23	3.77	4.084	1.40	(1.05)	6.59	3.505
1000	254.2	4.09	3.85	4.098	1.39	0.97	6.66	4.168
1100	252.4	4.06	3.87	4.112	1.40	0.95	6.68	4.835
1200	250.2	4.05	3.81	4.126	1.40	0.93	6.71	5.504
1300	248.7	4.04	3.83	4.140	1.40	0.90	6.73	6.175
1400	246.9	4.03	3.84	4.154	1.38	0.88	6.74	6.848
1500	245.1	4.03	3.86	4.168	1.40	0.86	6.75	7.522
1600	243.2	4.03	3.86	4.182	1.40	0.85	6.76	8.198
1700	241.4	4.03	3.86	4.196	1.40	0.83	6.77	8.874
1800	239.5	4.03	3.86	4.210	1.41	0.82	6.78	9.951

\* $K_S$  at 300 K from Yeganeh-Haeri (1994).

† $\delta_T = -(1/\alpha K_T)(\partial K_T/\partial T)_P$ .

‡ $\delta_S = -(1/\alpha K_S)(\partial K_S/\partial T)_P$ .

§ $K'_0(T) = K'_0 + 1.4 \times 10^{-4}(T - 300)$ .

# $\gamma = \alpha K_T V / C_V$ .

|| $q(T) = \delta_T - K'_0(T) + 1$  above  $T = \Theta$ .

\*\* $\Delta P_{Th} = P_{Th}(T) - P_{Th}(300)$ .

correct because of the omission of a small correction term, resulting from going from  $V$ - $T$  space to  $P$ - $T$  space. This term is  $(\alpha K_T / \partial T)_V \int_{T_0}^T \int_{T_0}^T \alpha dT dT$ . Jackson and Rigden (1996) in fact show in their Figure 6 that  $(\partial K_T / \partial T)_V$  is vanishingly small for  $T = \Theta$  and higher temperatures for MgSiO<sub>3</sub> perovskite (see also Fig. 9 of this report). It is a fraction of a percent between 300 and  $\Theta$ . The double integral term is large at high  $T$ , but it is severely depressed by the smallness of  $(\alpha K_T / \partial T)_V$  at high  $T$ . At low  $T$ , where  $(\partial K_T / \partial T)_V$  is just a few percent, the double integral term is small because of the value of  $\alpha$  and the smallness of  $T$ . The correction term was evaluated at all temperatures and found to be insignificant in the calculation of  $\Delta P_{Th}$ , so that Equation 13 is sufficient even though it is not rigorous.

The value of  $\Delta P_{Th}$  at 1800 K is 10 GPa for MgSiO<sub>3</sub> perovskite (Table 6). This is to be compared with  $\Delta P_{Th}(1800) = 9.24$  for Al<sub>2</sub>O<sub>3</sub> (Anderson and Isaak 1995), a value consistent with the change of  $\rho_0$  for the two solids. According to quasiharmonic theory, in the high- $T$  approximation, the value of  $\alpha K_T$ , which is the coefficient defined by  $(\partial P_{Th} / \partial T)_V$ , of silicates with an average mass of 20–21, should increase from mineral to mineral as  $\Theta^{4/3}$  (Anderson 1995). The increase in  $\Theta^{4/3}$  from Al<sub>2</sub>O<sub>3</sub> to MgSiO<sub>3</sub> perovskite is 5.5%; the increase in the high- $T$  value of  $\alpha K_T$  is about 5%. This means that the  $\Delta P_{Th}$ - $T$  relationship of MgSiO<sub>3</sub> perovskite fits nicely into the pattern of  $\Delta P_{Th}$  vs.  $T$  of rock-forming minerals (Fig. 2.3 in Anderson 1995). This constitutes a cross check on the value of  $\alpha K_T$  at high  $T$ .

**TABLE 7.** Isotropic sound velocities and Poisson's ratio

$T$ (K <sup>-1</sup> )	$\rho^*$ (g/cm <sup>3</sup> )	$v_{m\ddagger}$ (km/s)	$v_r\ddagger$ (km/s)	$v_s\§$ (km/s)	$v_p\#$ (km/s)	$\sigma_{  }$	$G^{**}$ (GPa)
300	4.104	7.272	6.57	8.00	11.04	0.224	177
400	4.094	7.230	6.53	7.97	10.97	0.226	175
500	4.087	7.187	6.49	7.94	10.92	0.227	172
600	4.084	7.142	6.45	7.91	10.86	0.228	170
700	4.068	7.104	6.41	7.88	10.82	0.229	167
800	4.051	7.066	6.38	7.86	10.77	0.230	165
900	4.045	7.022	6.34	7.82	10.71	0.231	163
1000	4.035	6.980	6.30	7.79	10.66	0.232	160
1100	4.028	6.936	6.26	7.75	10.60	0.232	158
1200	4.009	6.900	6.23	7.73	10.56	0.233	155
1300	3.993	6.861	6.19	7.70	10.51	0.234	153
1400	3.982	6.820	6.15	7.67	10.45	0.235	151
1500	3.971	6.778	6.12	7.63	10.39	0.235	149
1600	3.958	6.737	6.08	7.60	10.34	0.236	146
1700	3.951	6.694	6.04	7.56	10.28	0.237	144
1800	3.938	6.653	6.00	7.52	10.23	0.238	142

\*Calculated from  $V$  (Table 3, column 5).†Calculated from  $\Theta_D^E$  in Table 2 and Equations 3 and 5.

‡Calculated from Equation 5.

§Calculated from  $\sqrt{K_S/\rho}$ ;  $K_S$  from Table 6.#Calculated from  $v_p^2 = (K_S/\rho) + (4/3)v_s^2$ .||Calculated from  $v_s$  and  $v_p$  above.  $\sigma = [(v_p^2/v_s^2) - 2]/[2((v_p^2/v_s^2) - 1)]$ .\*\* $G$  calculated from  $G = \rho v_s^2$ .

Using Equation 13, Jackson and Rigden (1996) analyzed the  $PVT$  data of MgSiO<sub>3</sub> perovskite from four experiments (Ross and Hazen 1989; Wang et al. 1994; Utsumi et al. 1995; Funamori et al. 1996) and found thermal pressure vs.  $T$ . The variation of  $\Delta P_{Th}$  vs.  $T$  is shown by small circles in Figure 10, which is modified from Figure 5a of Jackson and Rigden (1996). Also plotted in this figure as a solid line is  $\Delta P_{Th}$  obtained in this study (listed in the last column of Table 6). In Figure 10, we observe that the calculated Debye value of  $\Delta P_{Th}$ , found in Table 6, is in agreement with that obtained from experiment, which means that for MgSiO<sub>3</sub> perovskite, the Debye model produces a satisfactory equation of state. In addition, when Equation 13 was replaced by the Mie-Grüneisen term for thermal pressure,

$$\Delta P_{Th} = \left(\frac{\gamma}{V}\right)[E_{Th}(T) - E_{Th}(T_0)] \quad (14)$$

(see Fig. 5b of Jackson and Rigden 1996), satisfactory agreement with experiment was also found.

#### CROSS CHECKS AND COMPARISON WITH OTHER REPORTS

##### $K_S$

$K_S$  was determined from the curve of  $(\partial K_S/\partial T)_p$  vs.  $T$  as taken from Jackson and Rigden's (1996) Figure 9.  $K_S$  could also have been calculated from  $K_S = K_T(C_p/C_v)$ , but I used this equation as a cross check. From Tables 2 and 4, at 1000 K,  $K_T(C_p/C_v) = 255.4$ , and from Table 6, as determined from Jackson and Rigden's (1996)  $(\partial K_S/\partial T)_p$ ,  $K_S = 254.2$ , off by 0.4%. The difference is 0.07% at 500 K. This cross check also constitutes a verification of the Jackson and Rigden (1996) calculations of  $K_S(T)$  and  $(\partial K_S/\partial T)_p$ .

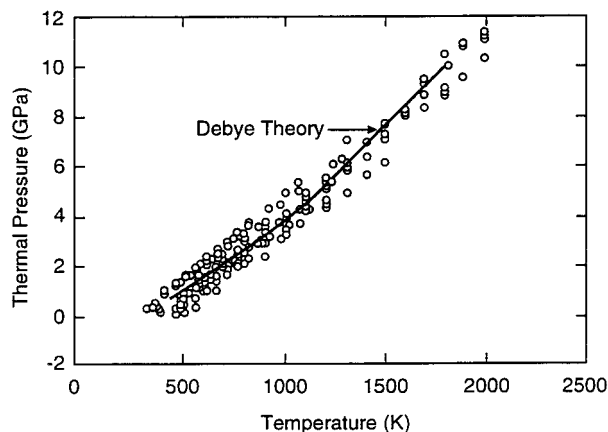


**FIGURE 10.** Thermal pressure vs. temperature for MgSiO<sub>3</sub> perovskite. The circles represent the database presented by Jackson and Rigden (1996), who analyzed experimental data from four reports. The solid line represents thermal pressure values found from the Debye model (Table 6) (figure adapted from Fig. 5a of Jackson and Rigden 1996).

##### $\delta_T$

I obtain  $\delta_T = 5.0$  at 300 K and 4.03 at  $T \geq \Theta$ . The steady change in  $\delta_T$  from  $300 < T < 1000$  and the constancy of  $\delta_T$  for  $T > \Theta$  agree well with what has been found for MgO, Al<sub>2</sub>O<sub>3</sub>, and Mg<sub>2</sub>SiO<sub>4</sub> (Anderson and Isaak 1995) (Fig. 11). The value,  $\gamma_0 = 1.5$  at 300 K, was found by Anderson et al. (1995a) in the comparison of isentropes of  $\rho$  vs.  $P$  for MgSiO<sub>3</sub> perovskite and the adiabat of the mantle, and  $\gamma_0 = 1.3$  at room temperature has also been reported by Gillet et al. (1996a).  $\delta_{T_0} = 5$  agrees reasonably well with the ambient measurements of Chopelas (1996), 4.3, who made spectroscopic measurements in the diamond cell. For measurements taken over a range of temperatures from 300 K upward,  $\delta_{T_0}$  should be lower than 5. Thus my results are consistent with the value determined by Anderson et al. (1996), 4.5, from the room-pressure, high-temperature measurement of Utsumi et al. (1995), 4.5, the Wang et al. (1994) value measured at 4.3, and the value 4.2 of Gillet et al. (1996a). At variance with this data is the report of Stixrude et al. (1992) that  $\delta_T \approx 7$ .

The value of  $\delta_T$  enables one to compute the value of  $\alpha$  at high pressure using the definition of  $\delta_T = -(\partial \ln \alpha / \partial \ln \rho)_T$ , which upon integration becomes

$$\left(\frac{\alpha}{\alpha_0}\right) = \left(\frac{\rho}{\rho_0}\right)^{-\delta_T} \quad (15)$$

Let us find  $\alpha$  at the conditions,  $P = 125$  GPa and 2500 K, where Gillet et al. (1996a) reported  $\alpha = 1.1 \times 10^{-5} \text{ K}^{-1}$ . At these conditions,  $\rho/\rho_0 = 5.49/4.08 = 1.345$ . The value of  $\delta_T$  at high  $T$  is 4.03, according to Table 6, and  $\alpha_0$  from the Gillet et al. (1996a) data (see Fig. 8) at 2500 K ( $P = 0$ ) is  $3.0 \times 10^{-5} \text{ K}^{-1}$ . From Equation 15,  $\alpha = 0.88 \times 10^{-5} \text{ K}^{-1}$ , which is below the Gillet et al. value. If we further consider the variation of  $\delta_T$  with volume,

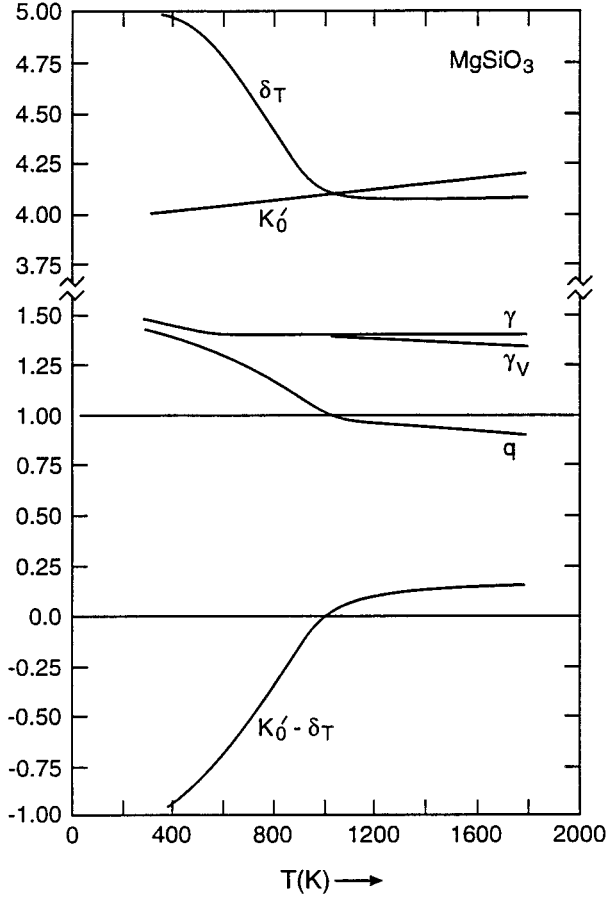


**FIGURE 11.** Plots of  $\delta_T$  and  $\delta_s$  vs.  $T$  for MgSiO<sub>3</sub> perovskite,  $\gamma = \alpha K_T V / C_V$ , and  $\gamma_V$  vs.  $T$  (all determined in this report).  $q = \delta_T - K'_0 + 1 + (\partial \ln C_V / \partial \ln V)_T$  and  $K'_0 - \delta_T$  are plotted.  $q = \delta_T - K'_0 + 1 + (\partial \ln C_V / \partial \ln V)_T$  shows that  $q = 1$  at  $T = 1000$  K and is close to unity elsewhere. The plot of  $K'_0 - \delta_T$  shows its resemblance to  $(\partial K_T / \partial T)_V$  in Figure 9.

the predicted  $\alpha$  is somewhat higher. Anderson and Isaak (1993) recommended that  $\delta_T$  change with  $(\rho/\rho_0)$  as  $\delta_T = \delta_{T_0}(\rho_0/\rho)^\kappa$ ; when placed in Equation 15, the aforementioned equation for  $\delta_T$  gives

$$\frac{\alpha}{\alpha_0} = \exp \left\{ -\frac{\delta_{T_0}}{\kappa} \left[ 1 - \left( \frac{\rho_0}{\rho} \right)^\kappa \right] \right\} \quad (16)$$

(Anderson and Isaak 1993). Anderson and Isaak (1993) found  $\kappa = 1.5$  for MgO, which agrees with the report by Gillet et al. (1996a) that ambient  $\delta_T$  decreases to 3.5 at 100 GPa. Using  $(\rho_0/\rho) = 0.740$  corresponding to 125 GPa,  $\kappa = 1.5$ , and the high- $T$  value 4.04 for  $\delta_T$ ,  $\alpha = 0.37\alpha_0$  or  $\alpha = 1.11 \times 10^{-5} \text{ K}^{-1}$ . This is a good match with the Gillet et al. (1996a) data point; I regard it as a satisfactory cross check on the value of  $\delta_T$  at high  $T$ , 4.03, found in this report. Using the value of  $\delta_T$  presented by Stixrude et al. (1992),  $\delta_T = 7$ , the value of  $\alpha$  at 125 GPa and 2500 K would by Equation 15 and by Equation 16 be unreasonably low.

$\gamma$

The steady descent of  $\gamma$  from 300 to 800 K and the subsequent value at high  $T$  being independent of  $T$  are consistent with the  $\gamma(T)$  behavior of other dense oxides (Anderson and Isaak 1995). The  $T = 300$  K value of  $\gamma$  found here, 1.52, is consistent with previous estimates that involved the author (Anderson and Masuda 1994; Anderson et al. 1995a). This is to be compared with the Chopelas (1996) value, 1.42, found from spectroscopic measurements in a diamond cell. At high  $T$ , the value of  $\gamma$  reported here is 1.4 and  $(\partial \gamma / \partial T)_p = 0$ . This value of  $\gamma$  is reasonably close to the high-temperature values of Wang et al. (1994) and Gillet et al. (1996a), who both found  $\gamma = 1.3$  from their measurements. Jackson and Rigden (1996) found  $\gamma = 1.33$  at high  $T$ . The Utsumi et al. (1995) data on  $V(T)$  lead to  $\gamma = 1.45$ , according to the analysis of Masuda and Anderson (1995). Stacey (1996) found  $\gamma = 1.30 \pm 0.09$  for the high- $T$  (2000 K) value of the perovskite structure by the classical method (displacement on pairs of neighboring atoms in the lattice is summed to obtain the net force and the resultant force is made equal to the thermal pressure).

There is, of course, the report by Hemley et al. (1992) that  $\gamma = 1.96(9)$ , which is at variance with the other reports listed above. It is conceivable that  $\gamma$  would be larger for an Fe-rich perovskite than for pure perovskite, but according to Anderson et al. (1996) a thermodynamic constraint prevents  $\gamma$  from being greater than  $0.5 K'_0 - 0.3$ . The Hemley et al. (1992) reported value of  $K'_0 = 3.9$  requires that  $\gamma < 1.6$ ; thus  $\gamma = 1.96(9)$  appears inconsistent with  $K'_0 = 3.9$ .

The Jackson and Rigden (1996) value of  $\gamma$ , 1.33, determined from a Mie-Grüneisen fit to the PVT data, is slightly less than that shown in Table 6, 1.40 at  $T = \Theta$ , which was calculated directly from  $\alpha$  and  $K_T$  through the definition,  $\gamma = \alpha K_T V / C_V$ , but this can be considered as good agreement.

$q$

As shown in Table 6 and Figure 7, the value of  $q$  is near unity and is exactly unity at 1000 K. Jackson and Rigden (1996) suggested that other properties are not sensitive to the exact value of  $q$ , so that  $q = 1$  was assumed. In this report I find that near  $T = \Theta$ ,  $q = 1$  is exact. Gillet et al. (1996a) found  $q = 1$ , but Hemley et al. (1992) reported  $q = 2.5(1.7)$ . Cynn et al. (1996) found that for Mg<sub>2</sub>SiO<sub>4</sub>,  $(\partial \ln C_V / \partial \ln V)$  rises steadily from 0 to 1 as  $T$  decreases from  $\Theta$  to 0. Using a straight line for interpolation, the values of  $(\partial \ln C_V / \partial \ln V)_T$  between  $0 < T < 1000$  were obtained, giving the values of  $q$  to be used in Equation 12 at low  $T$ . The values of  $q$  obtained using the interpolated values of  $(\partial \ln C_V / \partial \ln V)_T$  are shown in the parentheses of column 7, Table 6 (see Bina 1995 for a discussion of the uncertainty in  $q$  from previous studies).

$(\partial K_T / \partial T)_V$

A plot of this parameter vs.  $T$ , determined by Jackson and Rigden (1996), is shown in Figure 9.  $(\partial K_T / \partial T)_V$  can

also be determined by the data in Table 6 through the thermodynamic identity,

$$\left(\frac{\partial K_T}{\partial T}\right)_V \equiv \alpha K_T (K'_0 - \delta_T) \quad (17)$$

(see Anderson 1995, p. 57–58). Because  $\alpha K_T$  does not change significantly with  $T$  (neglecting the values at 400 K and 500 K),  $(\partial K_T/\partial T)_V$  should vary as  $K'_0 - \delta_T$ , which is plotted on the bottom of Figure 11. The resemblance between the curve  $(K'_0 - \delta_T)$  determined in this report and  $(\partial K_T/\partial T)_V$  determined by Jackson and Rigden (1996) (Fig. 9) constitutes a cross check on the values of  $\delta_T$ . The value of  $K'_0 - \delta_T$  vs.  $T$  from the curve in Figure 11 and the data for  $\alpha K_T$  in Table 6 yield, by Equation 17,  $(\partial K_T/\partial T)_V = -0.0044$  GPa/K at 300 K, whereas Jackson and Rigden (1996) reported  $(\partial K_T/\partial T)_V = -0.005$  GPa/K at ambient conditions. This excellent agreement constitutes a cross check on  $(\partial K_T/\partial T)_V$  as determined in this study.

### $(\partial P_{\text{th}}/\partial V)_T$

Because of the identity  $(\partial K_T/\partial T) \equiv -V[\partial(\alpha K_T)/\partial V]_T$ ,  $[(\partial \alpha K_T)/\partial V]_T$  vanishes when  $K'_0 - \delta_T = 0$ . But  $P_{\text{th}}$  is proportional to  $T$ , and  $(\partial P_{\text{th}}/\partial T)_p = \alpha K_T$ , so  $(\partial P_{\text{th}}/\partial V)_T$  also vanishes when  $\delta_T - K'_0$  vanishes (Anderson et al. 1992; Masuda and Anderson 1995). Anderson et al. (1995b) showed from a study on MgO that when  $\delta_T - K'_0 = \pm 0.2$ , the thermal pressure is, for all practical purposes, independent of volume. Figure 11 shows that from about 900 K up to 1800 K,  $K'_0 - \delta_T < |0.2|$ , so the thermal pressure of MgSiO<sub>3</sub> perovskite is independent of volume at high  $T$ . In this regard MgSiO<sub>3</sub> perovskite is like Al<sub>2</sub>O<sub>3</sub> and MgO (Anderson 1997). However, the value of the width of the volume zone necessary to satisfy  $(\partial P_{\text{th}}/\partial V)_T = 0$  is not apparent. Nevertheless for high temperatures it appears that one could safely assume that for a reasonably wide compression range, say for  $V/V_0$  between 1 and 0.9, the thermal pressure,  $P_{\text{th}}(V_0, T)$ , depends only on  $T$ , not on  $V$ . This means that the upper part of the curve in Figure 10 does not shift as the volume is changed.

## CONCLUSIONS

It is shown that MgSiO<sub>3</sub> perovskite is a Debye-like solid because the specific heat and entropy calculated to high  $T$  (1800 K) from Debye theory agree with available experimental data, especially those above 400 K. In this calculation, the thermal expansivity data of Funamori et al. (1996) and the acoustic velocity data of Yeganeh-Haeri (1994) are used as input. It is also shown that a number of thermoelastic properties, including  $(\partial K_T/\partial T)_p$ ,  $(\partial K_T/\partial T)_V$ ,  $K_T$ ,  $K_S$ ,  $\delta_T$ ,  $\delta_S$ ,  $\gamma$ ,  $q$ ,  $v_s$ ,  $v_p$ , and  $G$ , can be calculated and tabled up to high  $T$  once it has been proved that MgSiO<sub>3</sub> perovskite is a Debye-like solid. From the calculated properties,  $K_T$ ,  $K_S$ ,  $\gamma$ ,  $\rho$ , and  $(\partial K_T/\partial T)_V$ , the thermal pressure,  $\Delta P_{\text{th}}$ , can also be calculated to high  $T$ . When this is done, the resulting values of  $\Delta P_{\text{th}}$  are shown to agree with  $\Delta P_{\text{th}}$  calculated by Jackson and Rigden (1996) from the existing PVT data set. Thus for MgSiO<sub>3</sub> perov-

skite, Debye theory can be used to obtain the equation of state.

MgSiO<sub>3</sub> perovskite joins a small group of Debye-like minerals, now consisting of: MgO, Al<sub>2</sub>O<sub>3</sub>, and MgSiO<sub>3</sub> perovskite. For this group, the physical properties described above are calculated from data on acoustic sound velocities, ignoring the optic properties. The criterion for selection as a Debye-like solid is that the majority of optic modes occur at frequencies placed toward the center of the phonon density of states, e.g., the Debye frequency is larger in value than the frequencies of the majority of optic modes. By this criterion, other dense minerals, such as stishovite and MgSiO<sub>3</sub> ilmenite, are not likely candidates to be Debye-like solids.

Olivine is a near Debye-like solid. Guyot et al. (1996) showed that although Debye theory gives values close to experiment for the properties of  $C_V$ ,  $S$ , and  $\Delta P_{\text{th}}$  in olivine, the Kieffer approximation to the density of states gives values even closer to experiment.

## ACKNOWLEDGMENTS

The author acknowledges helpful conversations on several topics in this paper with Ann Chopelas, François Guyot, Guillaume Fiquet, Lars Stixrude, Russ Hemley, and Ian Jackson. I thank Philippe Gillet for editorial assistance and helpful comments on a previous version of this paper. John Carnes assisted with calculations on  $C_p$  and  $S$ . Overall calculations were checked by Judy Hohl using a spreadsheet. Supported by NSF grant EAR-96-14654. Support by ONR acknowledged. IGPP no. 4853.

## REFERENCES CITED

- Akaogi, M. and Ito, E. (1993) MgSiO<sub>3</sub> perovskite. *Geophysical Research Letters*, 20, 105–108.
- Anderson, O.L. (1963) A simplified method of calculating the Debye temperature from elastic constants. *Journal of Physics and Chemistry of Solids*, 24, 909–917.
- (1995) *Equations of state of solids for geophysics and ceramic science*. Oxford University Press, New York.
- (1997) The volume dependence of the thermal pressure of solids. *Journal of Physics and Chemistry of Solids*, 58, 335–343.
- Anderson, O.L. and Isaak, D.G. (1993) The dependence of the Anderson-Grüneisen parameter,  $\delta_T$ , upon compression at extreme conditions. *Journal of Physics and Chemistry of Solids*, 54, 221–227.
- (1995) Elastic constants of mantle minerals at high temperatures. In T.J. Ahrens, Ed., *Mineral physics and crystallography: A handbook of physical constants (Reference Shelf 2)*, p. 64–97. American Geophysical Union, Washington, D.C.
- Anderson, O.L. and Masuda, K. (1994) A thermoelastic method for computing thermal expansivity,  $\alpha$ , vs.  $T$  along isobars for silicate perovskite. *Physics of the Earth and Planetary Interiors*, 85, 227–236.
- Anderson, O.L. and Zou, K. (1989) Formulation of the thermodynamic functions for mantle minerals: MgO as an example. *Journal of Physics and Chemistry of Minerals*, 16, 642–648.
- Anderson, O.L., Isaak, D., and Oda, H. (1992) High-temperature elastic constant data on minerals relevant to geophysics. *Reviews of Geophysics*, 30, 57–90.
- Anderson, O.L., Masuda, K., and Guo, D. (1995a) Pure silicate perovskite and the PREM lower mantle model: A thermodynamic analysis. *Physics of the Earth and Planetary Interiors*, 89, 33–49.
- Anderson, O.L., Masuda, K., and Isaak, D.G. (1995b) A new thermodynamic approach for high-pressure physics. *Physics of the Earth and Planetary Interiors*, 91, 3–16.
- (1996) Limits on the value of  $\delta_T$  and  $\gamma$  for MgSiO<sub>3</sub> perovskite. *Physics of the Earth and Planetary Interiors*, 98, 31–46.
- Barron, T.H.K. (1955) Thermal expansion of solids at low temperatures. *Philosophical Magazine*, 7, 720–727.

- (1957) Grüneisen parameters for the equation of state of solids. *Annals of Physics*, 1, 77–89.
- (1977) Room temperature Debye-Waller factors of magnesium oxide. *Acta Crystallography*, A33, 602–604.
- Barron, T.H.K., Collins, J.G., and White, G.K. (1980) Thermal expansion of solids at low temperatures. *Advances in Physics*, 29, 609–730.
- Bina, C.R. (1995) Confidence limits for silicate perovskite equations of state. *Physics and Chemistry of Minerals*, 22, 375–382.
- Birman, J.L. (1984) *Theory of crystal space groups and lattice dynamics*, 538 p. Springer-Verlag, Berlin.
- Born, M. (1915) *Dynamik der Kristallgitter*, 1st Ed. Tuebner Press, Leipzig.
- (1923) *Atomtheorie der festen Zustandes*, 2nd Ed. Tuebner Press, Leipzig.
- Chopelas, A. (1990) Thermal expansion, heat capacity, and entropy of MgO at mantle pressure. *Physics and Chemistry of Minerals*, 17, 142–148.
- (1996) Thermal expansivity of lower mantle phase of MgO and MgSiO<sub>3</sub> perovskite at high pressure, derived from spectroscopy. *Physics of the Earth and Planetary Interiors*, 98, 3–16.
- Chopelas, A., Boehler, R., and Ko, T. (1994) Thermodynamics and behavior of  $\gamma$ -Mg<sub>2</sub>SiO<sub>4</sub> at high pressure: Implications for Mg<sub>2</sub>SiO<sub>4</sub> phase equilibrium. *Physics and Chemistry of Minerals*, 21, 351–359.
- Choudhury, N., Chapalet, S.L., Rao, K.R., and Ghose, S. (1988) Lattice dynamics of MgSiO<sub>3</sub> perovskite. *Pramāna Journal of Physics*, 30, 423–428.
- Cynn, H., Carnes, J.D., and Anderson, O.L. (1996) Thermal properties of forsterite, including  $C_v$ , calculated from  $\alpha K_T$  through the entropy. *Journal of Physics and Chemistry of Solids*, 11, 1593–1599.
- Debye, P. (1912) Zur Theorie der spezifischen Wärmen. *Annalen der Physik*, 39, 789.
- Funamori, N., Yagi, T., Utsumi, W., Kondo, T., and Uchida, T. (1996) Thermoelastic properties of MgSiO<sub>3</sub> perovskite determined by in situ x-ray observations up to 30 GPa and 2000 K. *Journal of Geophysical Research*, 101, 8257–8269.
- Gillet, P. (1996) Raman spectroscopy at high pressure and high temperature. Phase transitions and thermodynamic properties of minerals. *Physics and Chemistry of Minerals*, 23, 263–265.
- Gillet, P., Guyot, F., Price, G.D., Tournerie, B., and Le Cleach, A. (1993) Phase changes and thermodynamic properties of CaTiO<sub>3</sub>: Spectroscopic data, vibrational modelling and some insights on the properties of MgSiO<sub>3</sub> perovskite. *Physics and Chemistry of Minerals*, 20, 159–170.
- Gillet, P., Guyot, F., and Wang, Y. (1996a) Microscopic anharmonicity and equation of state of MgSiO<sub>3</sub>-perovskite. *Geophysical Research Letters*, 23, 3043–3046.
- Gillet, P., McMillan, P., Schott, J., Badro, J., and Grzechnik, A. (1996b) Thermodynamic properties and isotopic fractionation of calcite from vibrational spectroscopy of <sup>18</sup>O-substituted calcite. *Geochimica Cosmochimica Acta*, 60, 3471–3485.
- Guyot, F., Wang, Y., Gillet, P., and Ricard, Y. (1996) Quasi-harmonic computations of thermodynamic parameters of olivines at high-pressure and high-temperature. A comparison with experiment data. *Physics of the Earth and Planetary Interiors*, 98, 17–29.
- Hemley, R.J., Stixrude, L., Fei, Y., and Mao, H.K. (1992) Elasticity and equation of state of perovskite: Implications for the earth's lower mantle. In Y. Syono and M.H. Manghnani, Eds., *High pressure research: Applications to earth and planetary sciences*, p. 183–190. American Geophysical Union, Washington, D.C.
- Jackson, I. (1983) Some geophysical constraints on the chemical composition of the Earth's lower mantle. *Earth and Planetary Science Letters*, 62, 91–103.
- Jackson, I. and Rigden, S.M. (1996) Analysis of  $P$ - $V$ - $T$  data: Constraints on the thermoelastic properties of high-pressure minerals. *Physics of the Earth and Planetary Interiors*, 96, 95–112.
- Jeanloz, R. and Knittle, E. (1989) Composition of the lower mantle. *Philosophical Transactions of the Royal Society of London A*, 328, 377–389.
- Kieffer, S.W. (1982) Thermodynamics and lattice vibrations of minerals: 5. Applications to phase equilibria, isotopic fractionation, and high-pressure thermodynamic properties. *Reviews of Geophysics and Space Physics*, 20, 827–849.
- (1985) Heat capacity and entropy. In *Mineralogical Society of America Reviews in Mineralogy*, 14, 65–126.
- Kittel, C. (1971) *Introduction to solid state physics* (4th edition), 617 p. Wiley, New York.
- Knittle, E., Jeanloz, R., and Smith, G.L. (1986) The thermal expansion of silicate perovskite and stratification of the Earth's mantle. *Nature*, 319, 214–216.
- Liebermann, R.C. (1982) Elasticity of minerals at high pressure and temperature. In W. Schreyer, Ed., *High pressure researches in geosciences*, p. 1–14. Schweizerbart'sche, Stuttgart.
- Lu, R., Hofmeister, A.M., and Wang, Y. (1994) Thermodynamic properties of ferromagnesian silicate perovskites from vibrational spectroscopy. *Journal of Geophysical Research*, 99, 11,795–11,804.
- Mao, H.K., Hemley, R.J., Fei, Y., Shu, J.F., Chen, L.C., Jephcoat, A.P., Wu, Y., and Bassett, W.A. (1991) Effect of pressure, temperature and composition on lattice parameters and density of (Fe,Mg)SiO<sub>3</sub> perovskite to 30 GPa. *Journal of Geophysical Research*, 96, 8069–8079.
- Masuda, K. and Anderson, O.L. (1995) The isentropic density profile of perovskite computed by the thermal pressure. *Geophysical Research Letters*, 22, 2211–2214.
- Navrotsky, A. (1989) Thermochemistry of perovskites. In A. Navrotsky and D.J. Weidner, Eds., *Perovskite: A structure of great interest to geophysics and materials science*, p. 67–80. Geophysics Monograph 45, American Geophysical Union, Washington, D.C.
- Poirier, J.P. (1991) *Introduction to the physics of the earth's interior*, 261 p. Cambridge University Press, Cambridge.
- Ross, N.L., and Hazen, R.M. (1989) Single crystal x-ray diffraction study of MgSiO<sub>3</sub> perovskite from 77 to 400 K. *Physics and Chemistry of Minerals*, 16, 415–420.
- Sangster, M.J.L., Peckham, G., and Saunderson, D.H. (1970) Lattice dynamics of magnesium oxide. *Journal of Physical Chemistry*, 3, 1026–1036.
- Saxena, S.K., Chatterjee, N., Fei, Y., and Shen, G. (1993) Thermodynamic data on oxides and silicates, 297 p. Springer-Verlag, Berlin, Heidelberg.
- Shankland, T.J. (1972) Velocity-density systematics: Derivation from Debye theory and the effect of ionic size. *Journal of Geophysical Research*, 77, 3750–3758.
- Stacey, F.D. (1996) Thermoelasticity of (Mg,Fe)SiO<sub>3</sub> perovskite and a comparison with the lower mantle. *Physics of the Earth and Planetary Interiors*, 98, 65–78.
- Stixrude, L., Hemley, R.J., Fei, Y., and Mao, H.K. (1992) Thermoelasticity of silicate perovskite and magnesiowüstite and stratification of the earth's mantle. *Science*, 257, 1099–1101.
- Utsumi, W., Funamori, N., Yagi, T., Ito, E., Kikegawa, T., and Shimomura, O. (1995) Thermal expansivity of MgSiO<sub>3</sub> perovskite under high pressures up to 20 GPa. *Geophysical Research Letters*, 22, 1005–1008.
- Wang, Y., Weidner, D.J., Liebermann, R.C., and Zhao, Y. (1994)  $P$ - $V$ - $T$  equation of state of (Mg,Fe)SiO<sub>3</sub> perovskite: Constraints on composition of the lower mantle. *Physics of the Earth and Planetary Interiors*, 83, 13–40.
- White, G.K. and Anderson, O.L. (1966) Grüneisen parameter for magnesium oxide. *Journal of Applied Physics*, 430–433.
- Winkler, B. and Dove, M.T. (1992) Thermodynamic properties of MgSiO<sub>3</sub> perovskite derived from large scale molecular motions. *Physics and Chemistry of Minerals*, 18, 407–415.
- Yeganeh-Haeri, A. (1994) Synthesis and reinvestigation of the elastic properties of single crystal magnesium silicate perovskite. *Physics of the Earth and Planetary Interiors*, 87, 111–121.
- Zhao, Y. and Anderson, D.L. (1994) Mineral constraints on the chemical composition of the Earth's lower mantle. *Physics of the Earth and Planetary Interiors*, 85, 273–292.

MANUSCRIPT RECEIVED MARCH 18, 1997

MANUSCRIPT ACCEPTED AUGUST 22, 1997